

NUMERICAL HOMOGENIZATION OF FIBER-REINFORCED COMPOSITES WITH COMPLEX MICROSTRUCTURAL FEATURES

MAREK ROMANOWICZ

Bialystok University of Technology, Department of Mechanical Engineering, Bialystok, Poland

e-mail address: m.romanowicz@pb.edu.pl

A micromechanical model for solution of the problem of transverse stiffness of unidirectional fiber reinforced composites taking into account the presence of the interphase and a random distribution of fibers over the transverse cross-section has been developed. The influence of interphase properties on the elastic modulus in the transverse direction of glass/epoxy composites has been investigated. It has been found that numerical computations of transverse Young's modulus obtained from the unit cell models for different fiber volume fractions are in a good agreement with experimental data.

Key words: fiber-reinforced composites, micro-mechanics, finite element analysis

1. Introduction

The third phase between original constituents of a composite, known as an interphase, forms as a result of irreversible chemical reaction in the processing of thermosetting-matrix composites. It has been observed by using the atomic force microscope nanoindentation that the interphase has spatially varying rather than uniform properties (Gao and Mader, 2002). It is difficult to investigate experimentally the effect of such thin interphases between fibers and a matrix on composite properties. An alternative, or at least a complement to experimentation, is making use of numerical micromechanical models which take into account the presence of the interphase. Application of a representative unit cell approach in the modeling of the interphase is based on the assumption that it is possible to isolate a small volume element of a composite that is statistically representative of the material as a whole. Such an approach for the modeling of the elastic behavior of fiber reinforced composites with interphases was proposed by Wacker *et al.* (1998), Young and Pitchumani (2004) and Wang *et al.* (2006).

In the present study, both the inhomogeneous properties of the interphase and the random fiber distribution over the transverse cross-section are incorporated into a one micromechanical model. Application of such a unit cell in the modeling of the mechanical properties of fiber reinforced composites is novel. It can be expected that the consideration of these two aspects simultaneously allows us to identify the composite properties accurately.

2. Description of the micromechanical model

2.1. Unit cell

No manufacturing process can guarantee perfect uniformity of fiber placement in the composite volume. Therefore, the analysis of composites with a random microstructure is desirable. In this paper, the unit cell models of a randomly distributed fiber composite are generated using Wongsto and Li's algorithm (Wongsto and Li, 2005). The generation of a microstructure in this algorithm is based on disturbing an initially hexagonal periodic array of fibers packed in

a two-dimensional plane. The main input data are the number of fibers N , the fiber radius r_f and the fiber volume fraction V_f . A random angle α between 0° and 360° is first generated to determine the direction for the fiber to shift. Along this direction, a maximum possible distance of the shift d is found. Next, the second random number k is generated between 0 and 1, and the actual distance of shift is calculated as kd . This process is performed for every fiber to complete one iteration. The stirring of fibers terminates after the required number of iterations is completed and when the fiber volume fraction V_f in the central region of the unit cell is the same as in the outskirts region. Wongsto and Li's algorithm was implemented in Free Pascal programming language. Figure 1 shows a typical unit cell with $V_f = 0.52$ containing $N = 105$ fibers. Using an ANSYS finite element code, plain strain models made of isoparametric triangular finite elements with 6 nodes (PLANE183) were generated. It was assumed that perfect bonding between the matrix and the fibers exists. To ensure accurate displacement and stress field representation within each unit cell, sufficiently dense meshes consisting of approximately $2 \cdot 10^6$ elements with a quadratic displacement field approximation were used. The meshes comprised 400 elements equally spaced around the circumference of each fiber. It was found that such a discretization was fine enough to give accurate results from the numerical viewpoint and any increased mesh density provided no further accuracy in the solution obtained.

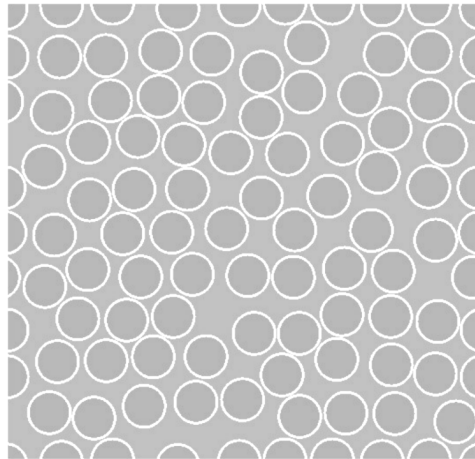


Fig. 1. Typical unit cell model with $N = 105$ fibers distributed at random for the fiber volume fraction $V_f = 0.52$

2.2. Interphase model

Following the approach by Anifantis (2000), it has been assumed that elastic properties of the interphase are non-uniform across its thickness and vary exponentially. The empirical relationships between the radial distance from the fiber boundary and elastic moduli of the interphase E_i , ν_i , are

$$\begin{aligned}
 E_i(r) &= E_m \left[1 + \left(p \frac{E_f}{E_m} - 1 \right) \frac{1 - \frac{r}{r_i} e^{1 - \frac{r}{r_i}}}{1 - \frac{r_f}{r_i} e^{1 - \frac{r_f}{r_i}}} \right] \\
 \nu_i(r) &= \nu_m \left[1 + \left(q \frac{\nu_f}{\nu_m} - 1 \right) \frac{1 - \frac{r}{r_i} e^{1 - \frac{r}{r_i}}}{1 - \frac{r_f}{r_i} e^{1 - \frac{r_f}{r_i}}} \right]
 \end{aligned}
 \tag{2.1}$$

where r denotes the radial component of the polar coordinate system whose origin is placed in the centre of a fiber, r_i and r_f are radii of the interphase and fiber, respectively. The factor q can be approximated by a function of the factor p , which, in turn, determines the bonding

conditions on the fiber surface and is defined by the ratio between the interphase modulus at $r = r_f$ and the fiber modulus

$$q = \frac{1 - \frac{\nu_f}{\nu_m}}{\left(\frac{E_f}{E_m} - 1\right) \frac{\nu_f}{\nu_m}} \frac{1 - p}{p} + 1 \quad (2.2)$$

where

$$p = \frac{E_i(r = r_f)}{E_f} \quad (2.3)$$

where $0 < p < 1$. Note, that a smaller p leads to a lower stiffness of the interphase. In numerical implementation, the radially graded interphase is discretized into 10 concentric layers characterized by homogeneous elastic properties as shown in Fig. 2.

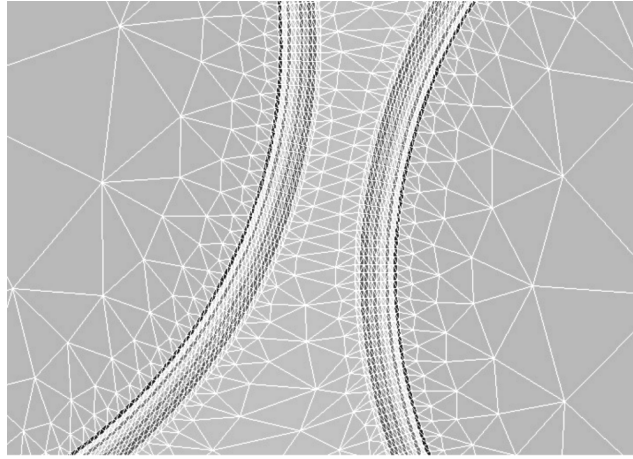


Fig. 2. Close-up view of the finite element mesh in the region of individual constituents

2.3. Model parameters

Numerical calculations have been performed for 3 different thicknesses of the interphase $t = 300, 500$ and 700 nm and 4 different fractions of the fiber volume $V_f = 0.333, 0.436, 0.531, 0.631$. In this paper, 5 different non-uniform distributions of the elastic moduli within the interphase characterized by factors $p = 0, 0.15, 0.30, 0.50, 1.00$ have been assumed for each value of t and V_f . Note, that when $p = 0$, a two-phase model is considered and no interphase occurs. And, in turn, when $p = 1$, a three-phase model without jumps in both elastic properties on the fiber surface is considered. Finite element computations have been carried out for a glass/epoxy composite reported by Wacker *et al.* (1998). The material parameters for the glass fibers sized by using the polyurethane binder (PU) and anhydride-cured epoxy resin (LY556/917) are summarized in Table 1.

Table 1. Properties of the constituent materials

Constituent	Properties
glass fiber (E-glass)	$E_f = 77$ GPa, $\nu_f = 0.2$, $r_f = 6$ μ m
epoxy resin (556/917)	$E_m = 3.11$ GPa, $\nu_m = 0.34$

2.4. Homogenization

According to Hill's principle (Hill, 1963), the volume average of the strain energy in a unit cell should be equal to the energy produced by the average strain and stress in an equivalent material

$$U = U^{eq} \quad (2.4)$$

where the strain energy of the equivalent material is given by

$$U^{eq} = \frac{1}{2} \int_V C_{ijkl} \Phi_{ij} \Phi_{kl} dV = \frac{1}{2} C_{ijkl} \Phi_{ij} \Phi_{kl} V \quad (2.5)$$

and the strain energy stored in the unit cell is as follows

$$U = \frac{1}{2} \int_V \sigma_{ij} \varepsilon_{ij} dV \quad (2.6)$$

where σ_{ij} , ε_{ij} are components of the microstress and microstrain, respectively, Φ_{ij} are components of the macrostrain and C_{ijkl} are components of the stiffness tensor. The elastic constants ν_{23} and E_2 are determined by applying normal components of the macrostrain to the unit cell, i.e. first Φ_{22} (state I), and next simultaneously Φ_{22} and Φ_{33} (state II). By using Eq. (2.4), an appropriate system of linear algebraic equations for the unknown stiffnesses can be formed. Under plane strain conditions, the solution for the stiffnesses is

$$C_{2222} = \frac{2U^I}{V(\Phi_{22}^I)^2} \quad C_{2233} = \frac{U^{II}(\Phi_{22}^I)^2 - U^{II}[(\Phi_{22}^{II})^2 - (\Phi_{33}^{II})^2]}{V(\Phi_{22}^I)^2 \Phi_{22}^{II} \Phi_{33}^{II}} \quad (2.7)$$

The relationships between the stiffnesses and the elastic constants are as follows

$$\nu_{23} = \frac{C_{2233}}{C_{2222} + C_{2233}} \quad E_2 = C_{2222} \frac{(1 + \nu_{23})(1 - 2\nu_{23})}{1 - \nu_{23}} \quad (2.8)$$

2.5. Boundary conditions

In the numerical homogenization, the periodic boundary conditions must be imposed on the unit cell to reflect the repeatability of the microstructure and to ensure the compatibility of the displacement fields. On the assumption of periodicity, each displacement field u_i may be decomposed in a linear part associated with the macrostrain Φ_{ij} and a periodic one u_i^p

$$u_i(x_1, x_2) = \Phi_{ij} x_j + u_i^p(x_1, x_2) \quad (2.9)$$

These relations are implemented at each periodic pair of nodes to link the displacements of the top and the bottom boundaries and the displacements of the right and left boundaries of the unit cell. Because of a huge number of nodes at the opposite boundary surfaces, a APDL program (Ansys, 2007) has been used to generate all required constraint conditions (2.9) automatically.

3. Validation of random fiber distribution

An efficient method of characterizing the regularity or irregularity in the distributions generated by this code is based on the computing of the pair distribution function $g(r)$ (Pyrz, 1994). This statistical function is defined as the probability of finding the centre of a fiber inside an annulus

of internal radius r and thickness dr with the centre at a randomly selected fiber. It can be expressed by the following equation

$$g(r) = \frac{1}{2\pi r} \frac{dK(r)}{dr} \quad (3.1)$$

where $K(r)$ is the second order intensity function. It gives the average number of fiber centroids expected to lie within the radius r about an arbitrary fiber centroid. For observations within the finite window of area A , the second order intensity function is defined as (Pyrz, 1994)

$$K(r) = \frac{A}{N^2} \sum_{k=1}^N \frac{I_k(r)}{R_p} \quad (3.2)$$

where N is the number of fibers within A , $I_k(r)$ is the number of fiber centroids within a circle of the radius r not counting the central fiber, and R_p is the ratio of the circumference of a circle of the radius r inside the viewing area to the entire circumference. For regular fiber distributions, $g(r)$ takes very sharp peaks and strongly oscillates with r . For random fiber distributions, on the other hand, $g(r)$ approaches a constant value of 1 as r increases.

4. Results and discussion

In Figs. 3 and 4, comparative analyzes of $g(r)$ in dependence on the non-dimensional radial distance are presented for two fiber volume fractions about 40% and 60%. The results presented in these figures are obtained by the averaging over 10 samples containing $N = 39, 105$ and 538 fibers. The comparison reveals that the code used in the present paper is, in general, able to produce random fiber distributions. Due to edge effects, the condition that $g(r) = 1$ as r increases cannot be fully satisfied for small N . Although, the fiber arrangements for small V_f and large N are more homogeneous and statistically valid, a tendency toward the random fiber distribution is visible for all tested samples. Therefore, taking the above into account, the unit cells involving the number $N = 105$ have been chosen for further study.

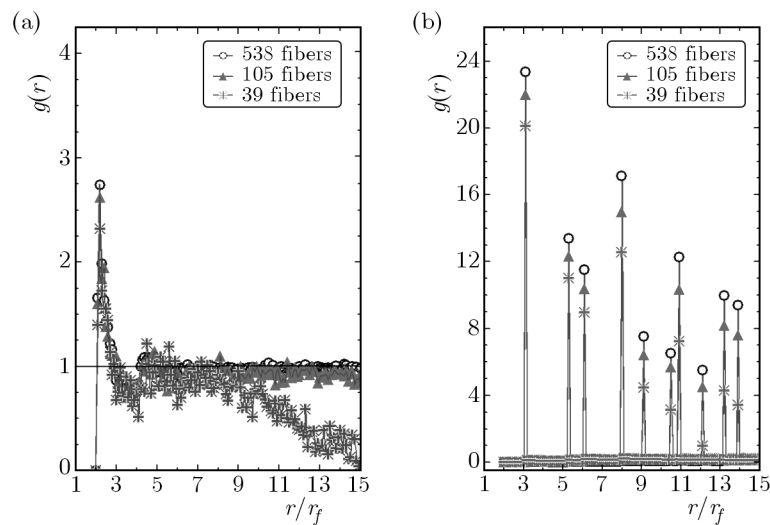


Fig. 3. Variation of the pair distribution function $g(r)$ with normalized radius r/r_f for the fiber volume fraction about 40%; (a) random fiber arrangement; (b) initial hexagonal fiber arrangement

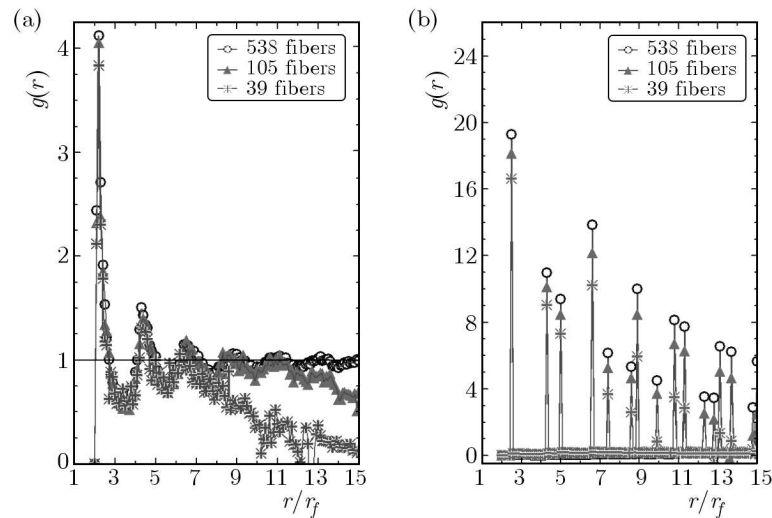


Fig. 4. Variation of the pair distribution function $g(r)$ with normalized radius r/r_f for the fiber volume fraction about 60%; (a) random fiber arrangement; (b) initial hexagonal fiber arrangement

The numerical calculations of transverse Young's modulus in dependence on the fiber volume fraction for the glass/epoxy composite with three values of the thickness of the interphase are presented in Figs. 5-7. In order to validate the numerical results, transverse Young's moduli obtained through the unit cell models have been compared to the experimental data reported by Wacker *et al.* (1998). It can be seen from these figures that the interphase parameters t and p have the significant effect on transverse Young's modulus. Note, that unit cell models without the interphase ($p = 0$) always produce unreliable results that lie under experimental points. For the case of models of too thin interphase (Fig. 5), numerical points have been also found to localize under experimental points even for an extremely stiff interphase ($p = 1$). Models with the interphase of a moderate thickness (Fig. 6) guarantee that mean values of the experimental moduli lie within the range of p from 0 to 1. For the case of models of a thick interphase (Fig. 7), not only the mean values but also standard deviations of the means are within this scope. Thus, the interphase with $t = 700$ nm is the most reliable. For the thickness $t = 700$ nm, the models with the interphase parameters $p = 0.15$ and 0.30 are in a very good agreement with the mean values of experimental data.

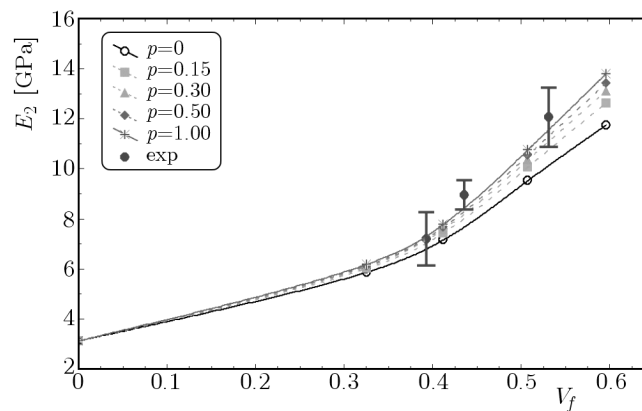


Fig. 5. Comparison between the model predictions for $t = 300$ nm and the experimental data (Wacker *et al.*, 1998)

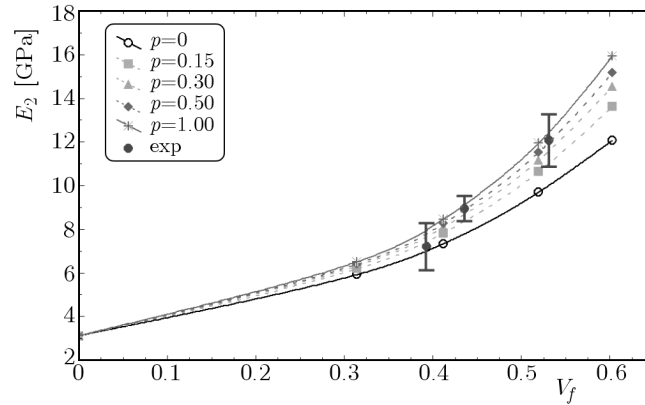


Fig. 6. Comparison between the model predictions for $t = 500$ nm and the experimental data (Wacker *et al.*, 1998)

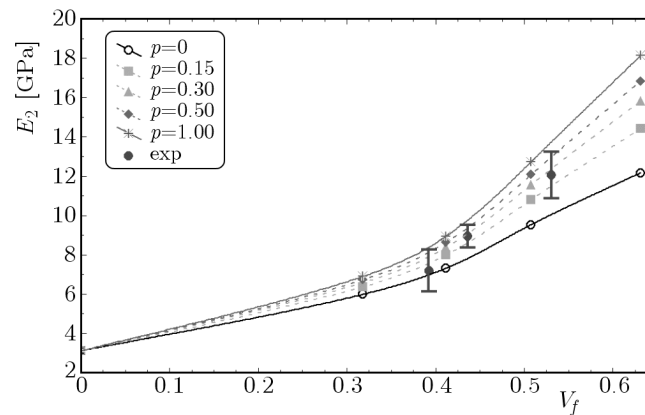


Fig. 7. Comparison between the model predictions for $t = 700$ nm and the experimental data (Wacker *et al.*, 1998)

5. Concluding remarks

By using the unit cell approach and the finite element method, a micromechanical model of fiber-reinforced composite for predicting transverse Young's modulus has been proposed. In particular, the effect of complex features such as the presence of the third phase between the reinforcement and the matrix and its inhomogeneous as well as the random distribution of the fibers over the transverse cross-section have been incorporated into the model. Also, a method of identifying the interphase properties has been presented and validated by comparison with the experimental data.

Acknowledgments

The financial support of the National Science Centre of Poland under contract DEC-2011/03/D/ST8/04817 is thankfully acknowledged.

References

1. ANIFANTIS N.K., 2000, Micromechanical stress analysis of closely packed fibrous composites, *Composites Science and Technology*, **60**, 1241-1248
2. ANSYS 11, 2007, *ANSYS Users's Manual*, Cannonsburg, PA

3. GAO S.L., MADER E., 2002, Characterization of interphase nanoscale property variations in glass fibre reinforced polypropylene and epoxy resin composites, *Composites Part A*, **33**, 559-576
4. HILL R., 1963, Elastic properties of reinforced solids: some theoretical principles, *Journal of the Mechanics and Physics of Solids*, **11**, 357-372
5. PYRZ R., 1994, Correlation of microstructure variability and local stress field in two-phase materials, *Materials Science and Engineering A*, **177**, 253-259
6. WACKER G., BLEDZKI A.K., CHATE A., 1998, Effect of interphase on the transverse Young's modulus of glass/epoxy composites, *Composites Part A*, **29**, 619-626
7. WANG J., CROUCH S.L., MOGILEVSKAYA S.G., 2006, Numerical modeling of the elastic behavior of fiber-reinforced composites with inhomogeneous interphases, *Composites Science and Technology*, **66**, 1-18
8. WONGSTO A., LI S., 2005, Micromechanical FE analysis of UD fibre-reinforced composites with fibres distributed at random over the transverse cross-section, *Composites Part A*, **36**, 1246-1266
9. YANG F., PITCHUMANI R., 2004, Effects of interphase formation on the modulus and stress concentration factor of fiber-reinforced thermosetting-matrix composites, *Composites Science and Technology*, **64**, 1437-1452

Manuscript received November 28, 2012; accepted for print February 14, 2013